Proceedings of the 2012 ACM Genetic and Evolutionary Computation
Conference (GECCO), Philadelphia, Pennsylvania, USA, July 2012.

Evolving Flexible Joint Morphologies

Jared M. Moore and Philip K. McKinley
Department of Computer Science and Engineering
Michigan State University
East Lansing, Michigan, USA
moore112@msu.edu

ABSTRACT

Transferring virtual robotic designs into physical robots has become possible with the development of 3D printers. Accurately simulating the performance of real robots in a virtual environment requires modeling a variety of conditions, including the physical composition of the robots themselves. In this paper, we investigate how modeling material flexibility through the use of a passive joint affects the resulting arm morphology and gait of a crawling virtual robot. Results indicate that flexibility can be a beneficial characteristic of robotic morphology design while also providing insight into the benefits of modeling material properties in a simulation environment.

Categories and Subject Descriptors

I.2.9 [**Computing Methodologies**]: Artificial Intelligence—*Robotics*

General Terms

Experimentation

Keywords

Evolutionary Robotics, Morphology, Morphological Evolution, Simulation

1. INTRODUCTION

The field of evolutionary robotics has produced many effective robotic designs that address a variety of tasks. Previous works have focused on controller evolution [1, 3, 5, 6, 7, 15, 23, 32], morphological evolution [11, 16, 29], and the co-evolution of morphology and control [7, 31] in virtual simulated environments. In some cases, these designs have been transferred into real robots for validation [14, 18, 24]. Designing robots with morphologies capable of accomplishing different tasks has presented both technical design and fabrication challenges. Recent developments in 3D printer technology now enable the rapid fabrication of robotic designs at finer levels of detail. It is possible to evolve a design in simulation and validate the results in a real robot in a short period of time.

Despite their potential to advance the field, 3D printers bring their own set of issues, including how to model the properties of physical materials and their interactions with each other and the external environment. Early studies addressing this "reality-gap" [10, 22] found that evolving controllers only in simulation can lead to solutions that are not transferable due to exploitation of the simulation environment [24]. When considering the morphology of a robot, accurately modeling the material properties is a vital component for simulations. High fidelity simulations will allow for better representations of physical properties that can reduce the differences between simulation and reality.

As a first step in addressing the reality gap with respect to physical materials, we need to demonstrate that the relevant characteristics can be modeled and subjected to selective pressures. Using these physical properties, we may be able to simplify robotic designs in the future by exploiting the material properties themselves. Robots often contain motorized joints, powered by actuators, to move various parts in order to accomplish tasks. However, material flexibility makes *passive* joints possible, which can increase performance and simplify controller complexity, since they do not require a dedicated motor. Harnessing the inherent properties of passive joints such as flexibility and the restorative properties of a material may allow for unique characteristics to evolve that improve the efficiency of a robot.

In this paper, we investigate the property of material flexibility in a morphological evolution experiment by implementing a passive joint and evaluating its movement characteristics. Results indicate that passive flexibility is a potentially useful characteristic in morphological evolution. Solutions exhibiting both semi-flexible and flexible joints exhibit increased performance when compared to more rigid morphologies. The flexibility demonstrated in the evolved solutions appears to be realistic and can be transferred into physical robots. This work helps to address the reality gap and the use of 3D printers in fabricating evolved robotic designs. The background and related work are presented in Section 2. Section 3 provides an overview of the virtual robot used in this experiment, a discussion of the simulation environment, as well as a description of the evolutionary process used. Results from the experiment are presented in Section 4 with a discussion following in Section 5. Conclusions and future directions are discussed in Section 6.

GECCO'12, July 7-11, 2012, Philadelphia, Pennsylvania, USA.

2. BACKGROUND

Evolutionary computation borrows concepts from biology to address complex computational tasks. By employing a process of development similar to natural evolution, novel solutions to problems can be found through optimization directed by fitness functions. Although these fitness functions are normally provided by a researcher, the actual process of evolution is left to a combination of mutation, crossover, and selection operations in order to minimize human bias. Solutions discovered through evolutionary computation often yield results that would not have been considered using traditional engineering methods. In the field of evolutionary robotics [5, 10, 17, 28], evolutionary computation is used to develop the aspects of control of a robot, both at the individual and group level, as well to optimize physical structures comprising the morphology of the robot. Employing these evolutionary concepts has yielded robots capable of bipedal walking [4, 29] as well as other types of robots used in the study of biological organisms [18, 19, 20, 21].

Many evolutionary approaches to robotics address the development of controllers for fixed morphology robots. Utilizing concepts and control patterns found in biology, controllers often emulate the neural architecture of natural creatures [9, 12, 18, 19, 20, 21]. Such works have laid the foundation for many of the concepts currently in use and provided insight into how natural organisms' neural controllers function. Research on morphology has been conducted mostly by applying co-evolution, in which controllers and morphology have been evolved concurrently [8]. This model closely resembles natural evolution, as organisms do not evolve new structures or locomotion strategies independently. This approach typically starts from a very primitive template which evolves into a complex final form capable of locomotion and other behaviors [27, 30]. Studies using co-evolution have investigated movement patterns using a predesigned initial robot, which was then subjected to evolution and resulted in solutions capable of effective locomotion with unique body structures and controllers [2, 7]. These co-evolution experiments have shown promise in producing robots capable of executing both simple and complex tasks [11, 16].

The ultimate goal of evolutionary robotics is synthesis [25, 26], in which a machine is capable of creating other machines in a process that mimics natural evolution. Realizing this goal depends in part on being able to model physical material properties in a realistic manner in simulation. New issues related to bridging simulation and reality have emerged with the introduction of 3D printing technologies. The reality gap appeared when controllers were evolved in simulation and transferred to real systems [10, 22]. Koos et al. [24] recently introduced a simulation-reality disparity measure to account for the differences in performance between the virtual and physical worlds. Moving from simulation to reality can further be refined by developing accurate models for physical conditions such as friction, gravity and material properties. 3D printing technologies increase the need for accurate material modeling, as new types of morphologies are possible that exploit properties of the constituent materials. In this paper, one of the properties, material flexibility, is explored in a simulated robot morphology.

3. METHODS

This section describes the various components of the study. An overview of the virtual robot is presented followed by a discussion of the simulation environment. Finally, a description of the evolutionary process is presented along with a discussion of the experimental procedures.

Virtual Robot.

A depiction of the virtual robot used in this study is presented in Figure 1. *Oxudercinae*, an amphibious fish commonly referred to as the mudskipper, was the inspiration for this two-armed model. Crawling locomotion is achieved by movement of the arms in a circular pattern. Each arm is connected to the main body by a joint with two degrees of freedom, allowing for a circular path of motion while preventing rotation of the arm in the third dimension. The angle between the arm and body is fixed at 23 degrees throughout the range of motion. In this study, movement of the arms is synchronous with a constant rate of oscillation.

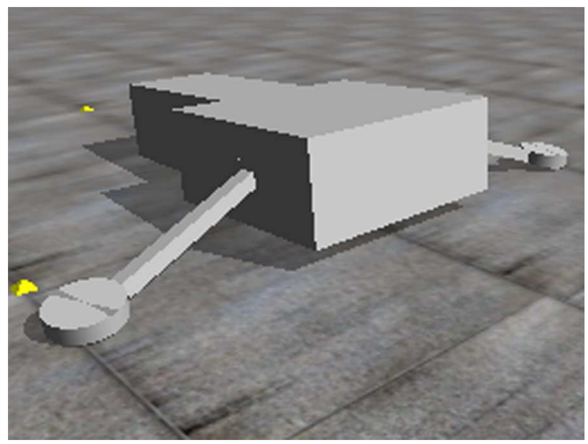

Figure 1: Initial morphology of the virtual robot. Body is fixed to accommodate motor and batteries in a real robot. The flexible joint is located between the arm and cylindrical foot. Different flexibilities allow for a variable contact area of the foot and ground.

Initial morphological design of the virtual robot was completed by hand allowing the body cavity to accommodate two motors and a battery required for realizing the robot in a real environment. Figure 2 depicts a prototype of the initial design that was printed using an Objet Connex 350 multi-material 3D printer. The prototype was printed to assess robot operation and properties of the constituent materials. Physical realization of the movement pattern required the use of two single-axle DC motors with a custom ball-and-socket joint interface with the arm. This design allowed for translating the rotational movement of the motor's drive shaft into an offset rotational motion. The initial prototype, upon which the virtual robot was based, was 14.8 centimeters long and 7.6 centimeters wide.

In the study described here, various aspects of the arm morphology are subjected to selective pressures to determine the most effective configuration for basic locomotion. The dimensional characteristics, arm length and foot radius are evolvable. Arm length is measured as the distance from

Figure 2: A hand-designed prototype of the robot produced with multiple materials. The feet are composed of both soft and rigid materials. This initial prototype had a completely rigid arm which resulted in a small contact area between the foot and surface during movement producing slippage of the feet on the surface.

the main body to the end of the foot. In the initial hand-designed robot, the joint between the arm and foot was not included and led to a rigid connection with a very small contact area between the arm and ground. This property created a higher chance of slippage when compared to a foot with an increased contact area. Flexibility is an important evolvable characteristic in this study and is modeled as a joint between the arm and foot. Two dimensions of flexibility are considered for this joint, enabling an ankle-like behavior. The flexibility of this joint determines what portion of the foot can come into contact with the ground potentially changing the amount of forward locomotion possible by the robot. In a flexible joint, the foot can come into full contact with the ground, maximizing the surface area, whereas, a rigid joint allows only for a very small part of the foot to contact the ground. Differing contact areas affect the traction that a robot is able to achieve, which can result in performance variation.

Simulation Environment.

A simulation using the Open Dynamics Engine (ODE) [13], was used to evaluate the performance of the various morphologies. The simulation parameters are presented in Table 1. Two separate environments were modeled using the simulator. In the primary environment, a flat plane was used with friction values set to approximate a slick surface, allowing for slippage of the feet during locomotion. The gravity and scale used in the simulation were set to model real world conditions. A secondary environment was introduced halfway through the evolutionary run that was also a flat plane. However, in this environment, friction values were set to be more like those found in a normal surface such as a countertop or floor, with a reduced chance of slippage due to the higher friction. Preliminary testing found that these two environments produced conflicting selective pressure upon the morphologies. Each individual was given 10 seconds of simulation time to travel as far as possible.

Table 1: The simulation parameters used in the experiment.

Parameter	Value
Timestep	.005 sec.
Evaluation Time	10 sec.
Primary Friction	0.6
Secondary Friction	1.0

Flexibility is modeled using two parameters, error reduction parameter (ERP) and constraint force mixing (CFM). Although these are simulation specific parameters, together they correlate to spring and damper constraints found in a mechanical model. ERP indicates the restorative force produced by a flexible joint that has moved away from its neutral position. This parameter ranges from 0 to 1, with values under 0.25 indicating that a minimal restorative force is applied to a deflected joint. In morphologies with these low values, the joint is returned to its neutral state only after the force that caused it to deform in the first place is removed. For example, in the simulation described here, the opposing force would be introduced when the foot comes into contact with the surface. A deflected foot would return to its neutral state only after the foot was no longer in contact with the surface. When ERP values exceed 0.25, a noticeable restorative force is present that returns a joint to its neutral position even as an opposing force is still acting upon the body.

The second component of flexibility is the CFM parameter, which determines how likely a joint is to move away from its neutral position. The value of CFM is strictly greater than 0. Generally, the larger the CFM value, the greater the joint will deflect under load. For purposes of this study, combinations of ERP less than 0.25 and CFM values greater than 0.8 resulted in flexible morphologies, while ERP values greater than 0.25 and CFM values greater than 0.8 resulted in morphologies that would be considered semi-flexible. In this paper, we consider flexible joints to be those that deformed upon contact with the ground and returned to a neutral state once the arm no longer was in contact with the surface. Semi-flexible joints were considered to be those that would deform upon contact with the surface but would return to neutral as the joint was still in contact with the ground. These semi-flexible joints can be thought of as a spring-like system in which the joint not only flexes to increase contact area, but also demonstrates a new component of the gait that is not present in fully rigid or flexible morphologies.

Evolutionary Setup.

Table 2 summarizes the parameters used for the evolutionary trials conducted in this study. Four separate treatments were conducted with 30 replicate runs each. With the exception of Treatment 1, a control with no evolution, each replicate run contained a population of 250 randomly generated individuals that were allowed to evolve for 100 generations. A simple genome was used in this study which contained the six parameters: arm length, foot radius, and ERP and CFM values for each of the two dimensions of the passive joint. A binary encoded genome was used for this study. Mutation and crossover operations were therefore subject to differing levels of impact depending on the location of the operation.

Crossover could occur at any point in the binary encoded genome. A representation of the genome can be seen in Figure 3. Selection was performed using a combination of elitism and tournament selection with a tournament size of 5. Specifically, the best performing individual per generation was carried over to the next generation with the remaining slots filled by tournament selection using parent individuals from the previous generation. Single-point crossover was used with a crossover probability of 20% and randomly selected crossover point using two parent solutions selected from the previous generation. Mutation was performed at the bit level with a probability of 2.3%, which equated to one mutation per genome.

Table 2: The evolutionary parameters used in the experiment.

Parameter	Value
Population Size	250
Generations	100
Replicate Runs	30
Tournament Size	5
Crossover Probability	20%
Mutation Rate	2.3%

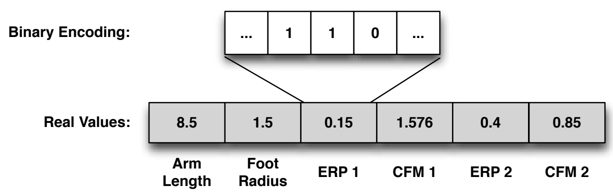

Figure 3: An example of the genome used in this study with sample values. Genome is encoded in binary values for purposes of mutation and crossover. As such, different mutation sites can result in higher or lower impact to the phenotype based on the position of the mutated bit.

Individual morphologies were evaluated by measuring the forward progress of the robot through the difference in the location of the main body segment at the start and finish of each individual replicate run. Equations (a) and (b) give the two fitness functions used in this experiment. For the first fifty generations, fitness was based only on performance in the primary environment as shown in Equation (a). Equation (b) was used for the simulations conducted after generation 50. Performance in these simulations was based on the forward progress from both environments which were added together and averaged to give a combined fitness value representing the two environments.

$$\text{fitness} = \text{prim\_fitness} \quad (a)$$
$$\text{fitness} = (\text{prim\_fitness} + \text{sec\_fitness}) \;/\; 2 \quad (b)$$

Experimental Setup.

Flexibility was evaluated through a set of four unique treatments that provide insight into its effect on a virtual robot's morphology and gait. The primary environment was a flat plane with low friction values. A secondary environment, introduced after 50 generations, was a similar flat plane with friction values more closely resembling that found on a normal surface. The two-environment approach is used to introduce competing pressures on the morphology. Introducing the secondary environment after 50 generations allows for a morphology to become near-optimal in one environment before being introduced to a different selective pressure from the second environment. This approach was based on the assumption that the robot is designed to perform tasks in a specific environment for the majority of its effective lifespan, occasionally interacting in a second type of environment. Once the second environment is introduced, fitness is treated as the average performance across both environments.

The evolvable parameters for each treatment are presented in Table 3. Treatment 1 is a control run that uses the initial hand-designed morphology prototyped prior to this study. The morphology of this creature is given an arm length of 8.5 centimeters and a foot radius of 1.0 centimeter with a rigid joint connecting the two parts of the arm. Flexibility of the passive joint is allowed to evolve in Treatment 2, while the dimensional characteristics of the arm morphology remain fixed at the values from Treatment 1. In Treatment 3, the dimensional characteristics of the arm morphology, arm length and foot radius, are placed under selective pressure while keeping the joint fixed. This run provides insight as to how morphologies evolve and perform without the influence of passive flexibility. Treatment 4 allows all aspects of the morphology to evolve under selective pressures providing feedback into how a complete morphology behaves in the two environments.

Table 3: Parameters subject to evolutionary pressure per treatment. X indicates a parameter subjected to selective pressures.

Parameters:	Arm Length	Foot Radius	Flexibility
Treatment 1			
Treatment 2			X
Treatment 3	X	X	
Treatment 4	X	X	X

4. RESULTS

Forward progress was the primary fitness measure used to assess the performance of the passive joint. Table 4 summarizes the fitnesses of the four treatments conducted in the study, providing the average forward progress achieved by each treatment in both environments along with the standard deviation, minimum, and maximum fitnesses found for the replicate runs. Treatments 2 and 3 have standard deviations of 0.0, as the replicate runs converged on similar performing solutions with small variations between the fitnesses of the replicate runs. Given the nature of these treatments, where at most one condition is subject to selective pressures, this is expected as there exists a small set of possible morphologies that optimize the fitness of the virtual robot. When more parameters were subjected to evolutionary pressures in Treatment 4, variation in the morphologies was seen with different competing morphologies gaining prevalence.

Table 4: Fitness summary for all treatments after the evolutionary runs.

Treatment:	1	2	3	4
Primary	26.8	28.3	32.0	44.6
Std. Dev.	0.0	0.0	0.0	0.1
Min.	26.8	28.3	32.0	42.9
Max.	26.8	28.3	32.0	46.5
Secondary	59.1	59.2	71.8	73.2
Std. Dev.	0.0	0.0	0.0	0.2
Min.	59.1	59.2	71.6	68.6
Max.	59.1	59.2	71.9	77.5
Distance traveled in cm.				

The average fitness for each treatment is presented visually in Figure 4. Error bars displayed in the graph are not visible for Treatments 1-3 as the variation in the replicate runs was minimal, however, Treatment 4 exhibits variation in performance in both environments. Performance in the secondary environment is significantly better than that of the primary environment, as the higher friction values found in the second environment allow the robot to move forward with less slippage. Evaluating the effect of flexibility on the performance of the various treatments is best seen by comparing Treatment 1 to Treatment 2 and Treatment 3 to Treatment 4. These comparisons demonstrate how a flexible joint performs against a rigid joint as well as how flexibility complements other aspects of morphology to improve performance.

When considering the effect of flexibility alone in Treatments 1 and 2, passive joints offer only a minimal improvement over a completely fixed arm morphology. In the primary environment, all trials in Treatment 2 performed better than Treatment 1, with an average improvement of 1.5 centimeters. Performance in the second environment was similar between the treatments. Greater friction rewards longer arms as opposed to a flexible joint in the secondary environment, explaining the lack of performance improvement for flexible joints. As the joint flexes, the effective arm length of the robot is reduced, resulting in a shorter distance of travel per arm stroke. Reviewing the resulting morphology of Treatment 2 showed a solution that uses a large restorative force to aid locomotion by giving the arm stroke an extra kick of the foot as the arm moved away from the ground. In this instance, the passive flexibility was directly responsible for an increase in the forward progress of the arm by exerting a force propelling the virtual robot forward.

Effect of flexibility on a fully evolvable morphology can be seen in the performance differences between Treatments 3 and 4. In the primary environment, an increased performance of at least 34% is achieved between the worst performing solution in Treatment 4 and the best performing solution in Treatment 3. Interestingly, the performance in the secondary environment is mixed, with some solutions performing worse than those with inflexible joints found in Treatment 3. These performance differences relate to the two different morphologies that became prevalent in the solutions for Treatment 4. Generally speaking, when friction is high, there is less pressure to increase contact area with the surface. Consequently, morphologies that are highly flexible tend to perform worse in the secondary environment due to the reduced effective arm length.

The evolved morphologies of the individual treatments exhibited similar dimensional morphology characteristics between replicate runs. Table 5 displays the morphological characteristic values found in this study. Treatments 2 and 3 generally resulted in replicate runs that evolved the same morphologies per treatment. The single evolvable traits in both treatments led to a single morphology giving optimal fitness. In Treatment 2, only flexibility is evolvable and Treatment 3 allows for evolving the dimensional morphological traits. Given these reduced parameters, evolution arrives at an optimal morphology relatively quickly. Treatment 4 yielded the most variable morphology likely due to the increased numbers of parameters that were subject to the evolutionary process.

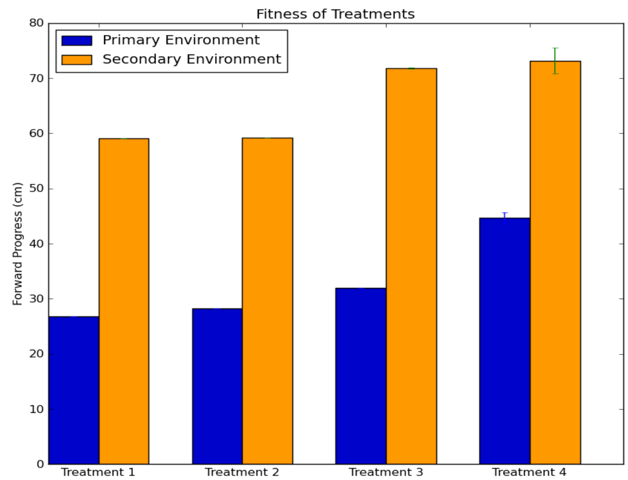

Figure 4: Forward progress of the various treatments in both environments. The primary environment fitness is generally lower due to the reduced friction environment resulting in increased slippage during locomotion.

When considering the morphologies that evolved in Treatment 4, two general patterns emerged. Figure 5 shows one of the solutions from Treatment 4, a morphology with high flexibility of the passive joint. This morphology tended to do well in the primary environment as it had a large contact area with the ground due to its high flexibility. However, the performance in the primary environment came at a cost, as the flexibility hindered performance in the secondary environment. A second morphology that came from Treatment 4 excelled in the secondary environment by having a semi-flexible morphology with a greater foot radius. These solutions utilized a small kicking motion of the foot during the period in which the foot contacted the ground to aid in propelling the robot forward. The joint did not deflect as far from the neutral position in these morphologies, which provided for a larger effective arm length than the highly flexible morphologies. This lower joint deflection resulted in the better performance observed in the secondary environment. Such behaviors illustrate the need for high fidelity simulations that account for the nuances of the constituent materials to better simulate material behaviors that can aid the performance of robots. In this case, the gaits of the dif-

Table 5: Evolved Morphology Characteristics

Attribute	Average	Std. Dev.	Min.	Max.
Treatment 1				
Attribute	Average	Std. Dev.	Min.	Max.
Arm Length	8.5	0.0	8.5	8.5
Foot Radius	1.0	0.0	1.0	1.0
No flexibility in this treatment.				
Treatment 2				
Attribute	Average	Std. Dev.	Min.	Max.
Arm Length	8.5	0.0	8.5	8.5
Foot Radius	1.0	0.0	1.0	1.0
ERP 1	0.767	0.000	0.767	0.767
CFM 1	1.968	0.000	1.938	1.984
ERP 2	0.100	0.000	0.100	0.100
CFM 2	2.307	0.136	2.16	2.6
Treatment 3				
Attribute	Average	Std. Dev.	Min.	Max.
Arm Length	10.275	0.000	10.275	10.275
Foot Radius	5.000	0.008	4.932	5.086
No flexibility in this treatment.				
Treatment 4				
Attribute	Average	Std. Dev.	Min.	Max.
Arm Length	10.275	0.000	10.275	10.275
Foot Radius	4.413	0.080	2.261	5.086
ERP 1	0.691	0.163	0.191	0.767
CFM 1	1.372	0.485	0.620	1.984
ERP 2	0.557	0.179	0.140	0.735
CFM 2	0.297	0.439	0.040	1.440

ferent morphologies benefitted from the small but important characteristics relating to flexibility. Increased simulation capabilities modeling these inherent material properties may result in further increases in robotic performance. Moreover, exploiting the properties of the constituent materials in this manner is complementary to other facets of robot design.

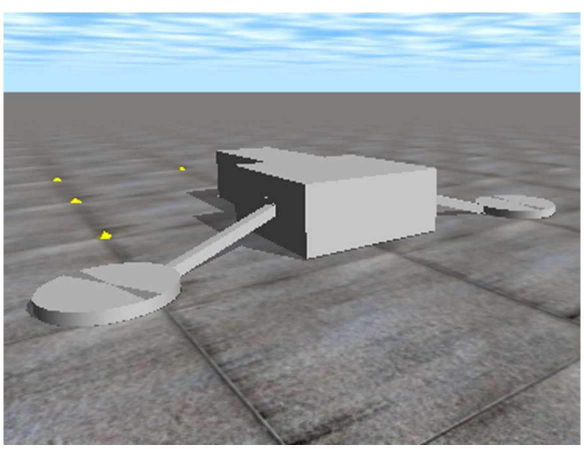

Figure 5: Evolved morphology demonstrating flexibility of the passive joint as it makes contact with the surface. In this morphology, the foot comes into full contact with the ground with the aid of a flexible joint at the arm-foot junction. The foot size also increased giving the morphology a greater contact area with the surface.

Further insight into the evolutionary process of Treatment 4 can be gained through Figure 6. The performance over evolutionary time is indicated for each environment by highlighting the best performing individual in a single environment and the best individual with respect to performance in both environments. Variation among the replicate runs is indicated by the error bars. The variation is due to the two different resultant morphologies that emerged over the course of this evolutionary run. In this case, the error bars also illustrate how the two separate general morphologies performed. When considering the secondary environment, the high error bar indicates solutions that utilized the semi-flexible morphology, as these excelled in the higher friction environment. The lower error bars indicate the solutions that harnessed more flexible morphologies to excel in the primary environment. For the primary environment lines, the inverse is true, with the high error bars indicating more flexible morphologies and the lower error bars indicating semi-flexible morphologies. This graph also demonstrates clearly the compromise made by the final solutions, in that the best performing individuals in one environment were not necessarily the solutions selected for their performance across both environments. The evolutionary path taken by the two morphologies is illustrated and provides insight as to how different morphologies can result from the same set of initial conditions to meet a fitness goal.

5. DISCUSSION

Visual observations of the behavior of the individual evolved solutions indicate that a variety of different flexibility characteristics arose in the final evolved morphologies for Treatment 4. The best performers in the primary environment had a combination of smaller foot radii and more flexible joints, enabling the feet to lie flat against the ground, increasing the contact area in the low friction environment. The majority of the solutions in Treatment 4 tended to evolve semi-flexible joints and larger foot radii to gain an advantage in the secondary environment, where performance gains were greater than those of the primary environment. Given the contribution of both environments to the fitness function, greater performance differences in the secondary environment results led to the semi-flexible morphologies being selected, as they performed better in a full friction environment. Regardless of the degree of flexibility evolved, all best performers selected in Treatment 4 exhibited at least a moderate amount of flexibility, with none of the trials resulting in an inflexible joint as the best performing individual.

Not only was flexibility beneficial to the virtual robots in this experiment, but the evolved solutions exhibited characteristics that is transferable to physical robots. Specifically, visual observation of the resulting evolved morphologies indicated that the solutions did not exploit flexibility in the simulation environment to develop unrealistic movement patterns, as has been noted in other research pertaining to the reality gap [10, 22, 24]. Transferring these designs into physical materials will require further analysis of material properties, but the initial findings of this study demonstrate that flexibility can be modeled adequately in a simulation environment. Of course, further verification will be necessary for new materials as the physical characteristics vary.

Modeling physical material properties in simulation can produce morphologies that make use of these characteristics to increase a robot's performance. Implementation of pas-

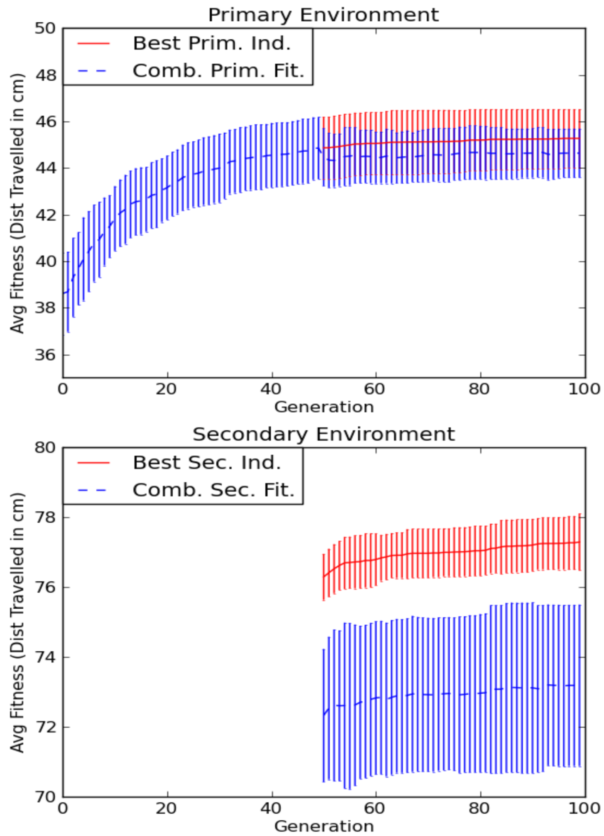

Figure 6: Treatment 4: Forward progress in both environments with all parameters subject to selective pressures. Compromise between the best individual in an environment and the individual morphology that is selected for its performance in both environments can be seen in the disparity between the two lines for each respective environment.

sive joints in physical robots could have positive effects such as increasing battery life and reducing weight due to the need for fewer motors. In the study described here, material flexibility aided the forward progress of the two resultant morphologies by either allowing the foot to increase its contact area with the ground, or by adding in a small kicking motion to aid in forward locomotion. These characteristics evolved through the use of evolutionary computation without the need for direct intervention during the testing phase. Providing a method for evolution to exploit these material properties may result in new characteristics emerging that increase performance in ways not considered *a priori*. It is therefore important to provide a simulation environment with the capabilities to make full use of these material properties when conducting evolutionary experiments concerned with morphology.

6. CONCLUSION

In this study, material flexibility was investigated through modeling the property in a virtual robot and evaluation in two separate simulated environments. The four treatments used in this experiment addressed passive joint flexibility both alone and coupled with dimensional characteristics of the arm morphology. Flexibility was found to be a beneficial characteristic, with evolved solutions exhibiting both semi-flexible joints that emphasized a forceful restorative force, and more pliable joints that increased the contact area with the ground. In the case of this study, evolved morphologies exhibited realistic characteristics that demonstrated the feasibility of modeling flexibility in a simulation environment. High quality simulations are necessary to model the material properties and allow evolution to incorporate these benefits into the morphological design of a robot.

Future experiments will refine the modeling of flexibility in passive joints. Additional work will focus on addressing material properties that help to close the reality gap. Further modeling of flexibility is planned in order to develop a more in-depth method of evaluating flexibility, such as devising a measure of flexibility based on deformation between parts. Using the capabilities of the 3D printer described earlier, fabricating evolved virtual robotic designs using the results of this study will help reduce the need for modification between simulated designs and physical realizations. Accurate simulation models will also allow for reduced transfer time between virtual and real robots.

7. ACKNOWLEDGMENTS

The authors gratefully acknowledge the contributions to this work of Anthony Clark, Jianxun Wang and Professor Xiaobo Tan. This research has been supported in part by National Science Foundation grants CNS-1059373, CNS-0915855, CNS-0751155, CCF-0820220, and DBI-0939454, and by U.S. Army Grant W911NF-08-1-0495. Any opinions, findings, and conclusions or recommendations expressed in this material are those of the author(s) and do not necessarily reflect the views of the National Science Foundation or other research sponsors.

8. REFERENCES

[1] J. Auerbach and J. C. Bongard. How robot morphology and training order affect the learning of multiple behaviors. In *Proceedings of the 2009 IEEE Congress on Evolutionary Computation*, pages 39–46, Trondheim, Norway, May 2009. IEEE.

[2] J. Auerbach and J. C. Bongard. Dynamic resolution in the co-evolution of morphology and control. In *Proceedings of the Twelfth International Conference on Artificial Life (ALIFE XII)*, pages 451–458, Odense, Denmark, 2010.

[3] J. Auerbach and J. C. Bongard. Evolving monolithic robot controllers through incremental shaping. In S. Doncieux, N. Bredeche, and J.-B. Mouret, editors, *New Horizons in Evolutionary Robotics*, volume 341 of *Studies in Computational Intelligence*, pages 55–65. Springer Berlin / Heidelberg, 2011.

[4] A. G. Baydin. Evolution of central pattern generators for the control of a five-link planar bipedal walking mechanism. *PALADYN Journal of Behavioral Robotics*, 2008.

[5] R. D. Beer and J. C. Gallagher. Evolving dynamical neural networks for adaptive behavior. *Adaptive Behavior*, 1(1):91–122, 1992.

[6] J. C. Bongard. Behavior chaining: Incremental behavioral integration for evolutionary robotics. In S. Bullock, J. Noble, R. Watson, and M. A. Bedau, editors, *Artificial Life XI: Proceedings of the Eleventh International Conference on the Simulation and Synthesis of Living Systems*, pages 64–71, Winchester, UK, 2008.

[7] J. C. Bongard. The utility of evolving simulated robot morphology increases with task complexity for object manipulation. *Artificial Life*, 16(3):201–223, 2010.

[8] J. C. Bongard and H. Lipson. Once more unto the breach: Co-evolving a robot and its simulator. In *Proceedings of the Ninth International Conference on the Simulation and Synthesis of Living Systems*, pages 57–62, Boston, MA, USA, 2004.

[9] V. Braitenberg. *Vehicles: Experiments in Synthetic Psychology*. The MIT Press, February 1986.

[10] R. A. Brooks. Artificial life and real robots. In F. J. Varela and P. Bourgine, editors, *Proceedings of the First European Conference on Artificial Life*, pages 3–10. MIT Press, Cambridge, MA, 1992.

[11] N. Chaumont, R. Egli, and C. Adami. Evolving virtual creatures and catapults. *Artificial Life*, 13(2):139–157, 2007.

[12] D. Cliff, P. Husbands, and I. Harvey. Explorations in Evolutionary Robotics. *Adaptive Behavior*, 2(1):73–110, June 1993.

[13] R. S. et al. Open Dynamics Engine, http://www.ode.org/, 2012.

[14] H. Feng and R. Wang. Construction of central pattern generator for quadruped locomotion control. In *Proceedings of the IEEE/ASME International Conference on Advanced Intelligent Mechatronics*, pages 979–984, Xi'an, China, July 2008. IEEE.

[15] D. Floreano, P. Husbands, and S. Nolfi. Evolutionary Robotics. In *Handbook of Robotics*. Springer Verlag, Berlin, 2008.

[16] P. Funes and J. Pollack. Evolutionary body building: Adaptive physical designs for robots. *Artificial Life*, 4(4):337–357, 1998.

[17] I. Harvey, E. D. Paolo, R. Wood, M. Quinn, and E. Tuci. Evolutionary robotics: A new scientific tool for studying cognition. *Artificial Life*, 11(1-2):79–98, 2005.

[18] A. Ijspeert, A. Crespi, and J. Cabelguen. Simulation and robotics studies of salamander locomotion. *Neuroinformatics*, 3(3):171–195, 2005.

[19] A. J. Ijspeert. A connectionist central pattern generator for the aquatic and terrestrial gaits of a simulated salamander. *Biological Cybernetics*, 84(5):331–48, May 2001.

[20] A. J. Ijspeert. Central pattern generators for locomotion control in animals and robots: A review. *Neural networks : The Official Journal of the International Neural Network Society*, 21(4):642–53, May 2008.

[21] K. Inoue, T. Sumi, and S. Ma. CPG-based control of a simulated snake-like robot adaptable to changing ground friction. In *Proceedings of the IEEE/RSJ International Conference on Intelligent Robots and Systems*, pages 1957 –1962, 2007.

[22] N. Jakobi. Running across the reality gap: Octopod locomotion evolved in a minimal simulation. In *Proceedings of the First European Workshop on Evolutionary Robotics: EvoRobot'98*, pages 39–58, Paris, France, 1998. Springer-Verlag.

[23] L. Konig and H. Schmeck. A completely evolvable genotype-phenotype mapping for evolutionary robotics. In *Proceedings of the Third IEEE International Conference on Self-Adaptive and Self-Organizing Systems*, San Francisco, California, 2009.

[24] S. Koos, J. B. Mouret, and S. Doncieux. Crossing the reality gap in evolutionary robotics by promoting transferable controllers. In *Proceedings of the 12th Annual Conference on Genetic and Evolutionary Computation*, GECCO '10, pages 119–126, New York, NY, USA, 2010. ACM.

[25] H. Lipson. Evolutionary robotics and open-ended design automation. In B. Cohen, editor, *Biomimetics*, pages 129–155. CRC Press, 2005.

[26] H. Lipson and J. B. Pollack. Automatic design and manufacture of robotic lifeforms. *Nature*, 406(6799):974–978, August 2000.

[27] M. Mazzapioda, A. Cangelosi, and S. Nolfi. Evolving morphology and control: A distributed approach. In *Proceedings of the 2009 IEEE Congress on Evolutionary Computation*, pages 2217–2224, Trondheim, Norway, May 2009. IEEE.

[28] S. Nolfi and D. Floreano. *Evolutionary Robotics: The Biology, Intelligence and Technology of Self-Organizing Machines*. The MIT Press, 2000.

[29] C. Paul and J. C. Bongard. The road less travelled: Morphology in the optimization of biped robot locomotion. In *Proceedings of the 2001 IEEE/RSJ International Conference on Intelligent Robots and Systems*, volume 1, pages 226 – 232, Maui, Hawaii, USA, 2001.

[30] L. Schramm, Y. Jin, and B. Sendhoff. Emerged coupling of motor control and morphological development in evolution of multi-cellular animats. In *Proceedings of the 10th European conference on Advances in artificial life: Darwin meets von Neumann - Volume Part I*, ECAL'09, pages 27–34, Berlin, Heidelberg, 2011. Springer-Verlag.

[31] K. Sims. Evolving 3d morphology and behavior by competition. *Artificial Life*, 1(4):353–372, 1994.

[32] T. Ziemke, N. Bergfeldt, G. Buason, T. Susi, and H. Svensson. Evolving cognitive scaffolding and environment adaptation: A new research direction for evolutionary robotics. *Connection Science*, 16(4):339–350, 2004.